

# Color Correction using 3D Gaussian Mixture Models

Miguel Oliveira<sup>\*</sup>, Angel D. Sappa<sup>‡</sup>, and Vitor Santos<sup>\*</sup>

<sup>\*</sup>Department of Mechanical Engineering, University of Aveiro,  
Campus Universitario Santiago 3800 Aveiro, Portugal

<sup>‡</sup>Computer Vision Center, Edifici O, Campus UAB,  
08193 Bellaterra, Barcelona, Spain  
{mriem,vitor}@ua.pt asappa@cvc.uab.es

**Abstract.** The current paper proposes a novel color correction approach based on a probabilistic segmentation framework by using 3D Gaussian Mixture Models. Regions are used to compute local color correction functions, which are then combined to obtain the final corrected image. The proposed approach is evaluated using both a recently published metric and two large data sets composed of seventy images. The evaluation is performed by comparing our algorithm with eight well known color correction algorithms. Results show that the proposed approach is the highest scoring color correction method. Also, the proposed single step 3D color space probabilistic segmentation reduces processing time over similar approaches.

**Keywords:** Color Correction, Gaussian Mixture Models, Image Mosaicing

## 1 Introduction

The photometrical correspondence between a pair of images is the object of study in this paper. In general, image mosaicing uses sets of images taken with the same lighting conditions and with a single camera, or similar ones. In this way, the colors present on both images are very similar and the problem of photometric correspondence is overlooked. The general problem of compensating the photometrical disparities between two geometrically registered images is referred to as color correction. This process is performed through the use of one or several *color transfer functions (ctf)* that use an image as a reference. In other words, color correction is the problem of adjusting the color palette of an image using information from the color palette of another image. The image that is used as a reference is referred to as the *source image*, while the image which is going to be adjusted is called the *target image*. Figure 1 shows the target (*a*) and source (*b*) images of a city landscape. In Fig. 1 (*c*) a mosaic of both is shown. Due to light and shadow variations, different sensors or vignetting effects from the lenses, the mosaicing of the images shows disparities in color. These disparities are solved using color correction methodologies.

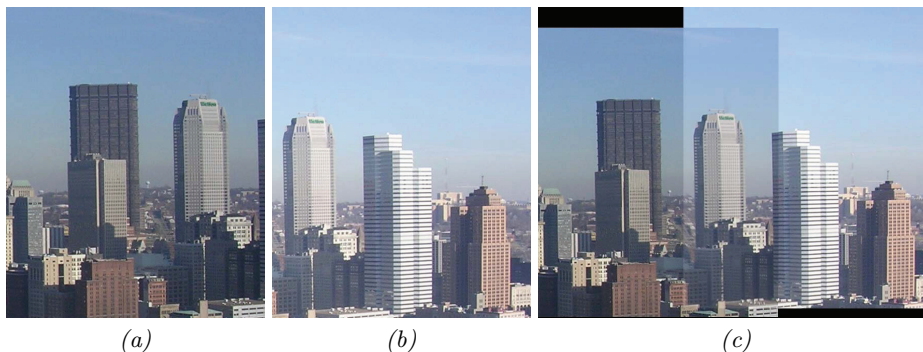


**Fig. 1.** A mosaic of two images of a city landscape scene (*c*). The colors of the target image (*a*) must be corrected using information from the source image (*b*) to avoid the artifacts present in the mosaic.

The problem of color correction has been widely studied during the last decade. Some authors suggested to solve this problem by using non parametric approaches, i.e., methods that make no assumptions about the nature of the color distribution. While some authors have attempted to model the radiometric response functions of the sensors and the exposures [10], others inclusively model the vignetting phenomenon [14] and there are some others that provide techniques to model the combination of both [5] [6]. This trend is usually addressed just for intensity images and so is not considered in color correction. In [3, 4], color correction is done through the estimation of global and local color transfer functions. The complex estimation problem is reduced to a robust 2D tensor voting in the corresponding voting spaces. A cumulative histogram matching technique was presented in [2], while in [7] the entire probability density function is mapped without making assumptions on its nature. On the other hand, model based parametric approaches try to model the color distribution in the images and use tools that transfer the color distribution characteristics from one image to the other. One of the most important works in this scope is [8]. In that paper, a simple statistical distribution transfer methodology was proposed. It was also in [8] that an alternative color model, namely the  $l\alpha\beta$  color-space, was proved to be more effective for calculating the color transfer functions than the usual RGB color-space. It is successfully employed since it minimizes the cross channel correlation, which is present on many color spaces. This work has been extended in [11], where tools that permitted RGB color space to be used with similar effectiveness were presented. Principal component analysis where implemented by [13]; while in [1] a gain compensation algorithm and a multi-band blending post processing was proposed.

The current paper proposes a new color correction technique based on 3D Gaussian Mixture Models ( $3DGMM$ ). To assess the effectiveness of the proposed algorithm, a very large set of images is used, and eight other state of the art algorithms for color correction are evaluated. The evaluation metric is taken from

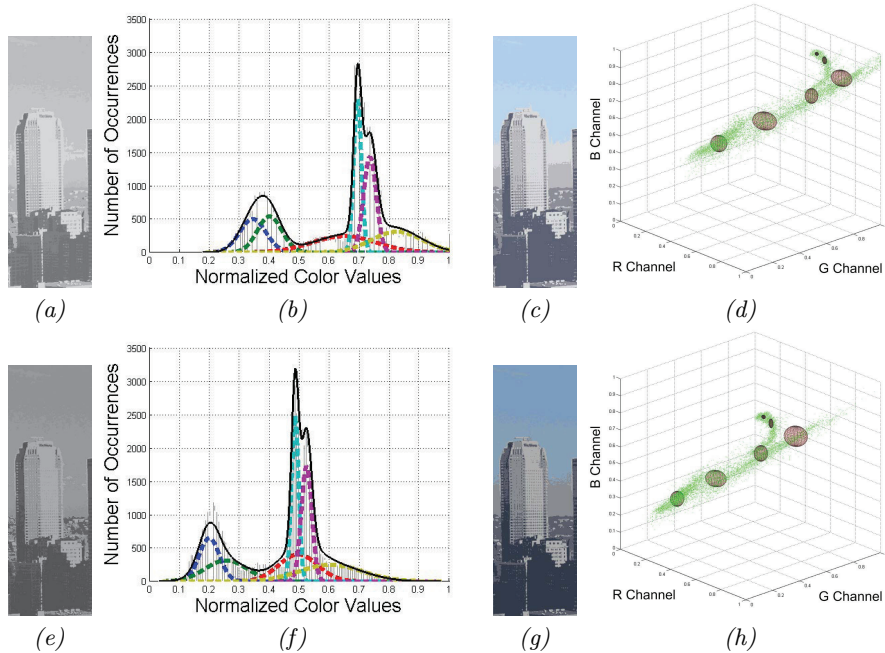


**Fig. 2.** Single channel color segmentation of the Source (a) and Target (e) images. Single channel histograms, Gaussian components (dashed) and total Gaussian mass (solid black) of the source (b) and target (f) images. 3D color segmentation of the source (c) and target (g) images. Color distribution of all pixels (green dots) and 3D Gaussian components (red ellipsoids) of the source (d) and target (h) images.

a recent performance evaluation of color correction algorithms [12]. Results show that the proposed approach is the best performing color correction algorithm.

The remainder of the paper is organized as follows. In section 2 the color correction technique based on 3D Gaussian Mixture Models (3DGMM) is presented. Results and comparisons are given in section 3. Finally, conclusions are presented in section 4.

## 2 Proposed Approach

The approach presented in [8] assumes a Gaussian distribution of color on both the source and target images, i.e., it uses a linear color transfer function. The Gaussian distribution based color transfer scheme, initially proposed in [8], can be defined as follows: let  $\mu_s$  and  $\mu_t$  be the mean color of the source and target images, while  $\sigma_s$  and  $\sigma_t$  are the standard deviations of the colors in those images. Then, the corrected image's color is given by the following Gaussian distribution transfer function:

$$c' = \mu_s + \frac{\sigma_s}{\sigma_t} \times (c - \mu_t), \quad (1)$$

where  $c'$  and  $c$  are the target image's original and new single channel color. Equation (1) may be used to process single channel images (*gain compensation*) or color images (*color correction*). For color images eq. (1) is applied separately for the three color channels. However, in practical situations, the color distribution of the whole image is seldom a normal distribution. Global modelling of the color distribution fails in practice because it provides only a rough approximation of the color distribution. By computing, for several regions, a local color transfer function and assuming a separate Gaussian distribution for each region, the set of color transfer functions will provide a more consistent color correction output. This was proposed in [9], where the Reinhard's methodology was extended to the local scenario, namely through a color transfer scheme based on single channel probabilistic segmentation and region mapping using the EM algorithm.

The current paper proposes to represent color distribution using *3DGMM* for joint probabilistic segmentation of the three color channels. Then, several color transfer functions can be derived from the adaptation of equation (1). The methodology consists of three stages and is detailed below.

## 2.1 Probabilistic Segmentation with 3DGMMs

The first stage consists of modelling the distribution of color in both images using Gaussian Mixture Models (GMMs). GMMs are among the most statistically mature methods for clustering. In this case they are used to model the color distribution of the pixels by segmenting the given image. After segmentation, each cluster is a Gaussian component from the mixture model. The following notation refers to the RGB color space. However, the presented method is not restricted to this color space. In fact, alternative color spaces have been tested, although results have shown no particular advantages when compared to the traditional RGB. This is because the joint color correction of the three color channels avoids cross channel artifacts, as detailed below.

Let  $NG$  be the number of Gaussian components that model the color distribution of an image. Let a given color be denoted as  $\mathbf{c} = [r, g, b]$ . A Gaussian component  $\omega_k$  has mean  $\boldsymbol{\mu}^k = [mean(r), mean(g), mean(b)]$  and standard deviation  $\boldsymbol{\sigma}^k = [std(r), std(g), std(b)]$ . The color distribution is modelled by the mixture of Gaussian components, so that the total density of pixels for a given color  $D(\mathbf{c})$  is given by the weighted sum of the Gaussians:

$$D(\mathbf{c}) = \sum_{k=1}^{NG} mp^k \times P^k(\mathbf{c}), \quad (2)$$

where  $mp^k$  is the mixture proportion of Gaussian component  $\omega_k$ , and  $P^k(\mathbf{c})$  is the probability of Gaussian  $\omega_k$  for color  $\mathbf{c}$ , which is given by the difference between two cumulative distribution functions of neighboring colors. The cumulative distribution function of Gaussian  $\omega_k$  for a given color  $\mathbf{c}$ , denoted as  $cdf(\omega_k, (c))$ , is given by:

$$cdf(\omega_k, \mathbf{c}) = \frac{\sum_{i=1}^3 \left( \frac{1}{2} \left( 1 + \operatorname{erf} \left( \frac{\mathbf{c}(i) - \boldsymbol{\mu}^k(i)}{\sqrt{2 \times (\boldsymbol{\sigma}^k(i))^2}} \right) \right) \right)}{3}, \quad (3)$$

where  $(i)$  is the index of the color channel (i.e.,  $i \in \{r, g, b\}$ ), and  $\operatorname{erf}$  is the error function, also known as probability integral, given as:

$$\operatorname{erf}(x) = \frac{2}{\sqrt{\pi}} \int_0^{\infty} e^{-x^2} dx. \quad (4)$$

Hence, the probability of the Gaussian component  $k$  is computed as:

$$P^k(\mathbf{c}) = cdf(\omega_k, \mathbf{c} + \boldsymbol{\lambda}) - cdf(\omega_k, \mathbf{c} - \boldsymbol{\lambda}), \quad (5)$$

where  $\boldsymbol{\lambda} = [cr/2, cr/2, cr/2]$  is given by half the image's color resolution ( $cr$ ).

In [9], each channel of the image undergoes a segmentation procedure similar to this one. However, in that approach, since the probabilistic segmentation is performed independently for each channel, the probabilities of Gaussian components may be different from channel to channel, i. e.,  $P^k(\mathbf{c}(1)) \neq (P^k(\mathbf{c}(2)) \neq (P^k(\mathbf{c}(3)))$ . The methodology proposed in the current paper uses a single probability function for all the three color channels, i.e.,  $P^k(\mathbf{c})$ , as defined in eq. (5). This reduces the occurrence of cross channel artifacts that arise from color correction as is the case in [9]. As will be shown in section 3, by performing a 3DGMM of all three image channels in a joint segmentation step we are able to improve the color correction performance and reduce processing time. Figure 2 shows the GMM color segmentation both for the 1D and the 3D cases.

## 2.2 Color Transfer Functions

The current paper proposes to perform a probabilistic segmentation of both the source and target images using 3DGMMs. The result of the segmentation step is that both the target and the source images are segmented into  $NG$  clusters, each representing a Gaussian component for the inferred mixture model. It is then necessary to associate each Gaussian component from the target image to another of the source image. This association is referred to as matching of Gaussian components. When spatial information exists, which is the case since images are registered, the matching is performed based on the maximum spatial correlation of pixel probabilities. To compute the spatial correlation, let  $color$  be the function that retrieves the color of a pixel. The probability  $P$  that each pixel  $\mathbf{x}$  has of belonging to Gaussian component  $\omega_k$  is calculated using the color retrieval function. For simplification purposes,  $P^k(color(\mathbf{x}))$  will be from now on denoted as  $P^k(\mathbf{x})$ . The matching of Gaussian components is computed as follows: let  $m(k)$  be the matching function that outputs the index of the source image Gaussian component for target image Gaussian component  $k$ :

$$m(k) = \operatorname{argmax}(r(k, j)), \forall j \in \{1, 2, 3, \dots, NG\}, \quad (6)$$

where  $r$  represents the spatial correlation between the probabilities of target image Gaussians  $P_t$  with source image Gaussians  $P_s$ , given by:

$$r(k, j) = \frac{\sum_{\mathbf{x}=[1,1]}^{[W,H]} (P_t^k(\mathbf{x}) - \bar{P}_t^k) \times (P_s^j(\mathbf{x}) - \bar{P}_s^j)}{\sqrt{\sum_{\mathbf{x}=[1,1]}^{[W,H]} (P_t^k(\mathbf{x}) - \bar{P}_t^k)^2 \sum_{\mathbf{x}=[1,1]}^{[W,H]} (P_s^j(\mathbf{x}) - \bar{P}_s^j)^2}}, \quad (7)$$

where  $\bar{P}^k$  represents the probability of the average color of Gaussian  $k$ , i.e.,  $\bar{P}^k = P(\boldsymbol{\mu}^k)$ , and  $W$ ,  $H$  are the image's width and height respectively.

The color correction procedure will make use of  $NG$  color transfer functions, each one corresponding to a match between a region in the target with a region in the source image. The color transfer functions (*ctf*) are obtained by adapting (1) to the 3D case:

$$ctf^{k,m(k)}(i) = \boldsymbol{\mu}_s^{m(k)}(i) + \frac{\boldsymbol{\sigma}_s^{m(k)}(i)}{\boldsymbol{\sigma}_t^k(i)} \times (\mathbf{c}(i) - \boldsymbol{\mu}_t^k(i)), \quad (8)$$

### 2.3 Color Correction

Once the source and target images have been segmented into  $NG$  regions and the corresponding color transfer functions for each match are computed, the objective at this last stage is to correct the color of every single pixel. Because of the probabilistic nature of the proposed color segmentation, pixels may have non zero probability of belonging to more than one region. Hence, the proposed color transfer approach is defined as a weighted combination of all the computed color transfer functions:

$$\mathbf{c}'(i) = \sum_{k=1}^{NG} mp^k \cdot P_t^k(\mathbf{c}) \cdot ctf^{k,m(k)}(i), \quad (9)$$

where the bold symbol  $\mathbf{c}'$  denotes the three channel color of the color corrected image and  $(i)$  is the index of the color channel.

## 3 Results

In order to test the proposed algorithm, the two data sets of a recent performance evaluation [12] were used. They consist of a synthesized data set of 40 image pairs and a real image data set of 30 image pairs. The registration of target / source was not provided by the authors of [12]. Because of this, a manual process of hand labelling pixels in both images was done to obtain the registration. In order to compare the results of the proposed approach with the state of the art, eight of the nine algorithms used in [12] were applied to the same data sets. Regarding

**Table 1.** Average and standard deviation of CS and SS scores for the two data sets. Average processing time per image is also provided. The proposed approach (# 10) obtains the highest average CS score.

Approach Reference	Alg. #	Synthetic					Real				
		CS		SS		Time (sec)	CS		SS		Time (sec)
		$\mu$	$\sigma$	$\mu$	$\sigma$		$\mu$	$\sigma$	$\mu$	$\sigma$	
Baseline	#1	18.66	3.92	1.00	0.00	—	16.44	3.40	1.00	0.00	—
Brown 07 [1]	#2	21.35	2.56	0.97	0.02	0.53	19.89	3.27	0.96	0.03	0.51
Xiao 06 [11]	#3	19.03	5.97	0.71	0.27	0.72	19.43	5.80	0.65	0.17	1.35
Reinhard 01 [8]	#4	19.86	4.92	0.79	0.15	0.43	20.25	6.78	0.67	0.17	0.94
Fecker 08 [2]	#5	26.79	6.04	0.90	0.06	0.93	21.93	4.07	0.89	0.10	1.64
Zhang 04 [13]	#6	26.29	6.65	0.91	0.07	0.70	20.41	3.56	0.87	0.13	0.93
Tai 05 [9]	#7	27.45	7.77	0.90	0.08	54.47	21.23	4.24	0.85	0.13	148.00
Jia 05 [4]	#8	27.71	7.33	0.91	0.06	233.50	21.82	4.05	0.85	0.17	235.70
Kim 08 [5]	#9	27.82	7.58	0.90	0.06	5.93	21.85	4.03	0.88	0.10	6.92
<b>this paper</b>	<b>#10</b>	<b>28.18</b>	<b>4.11</b>	<b>0.74</b>	<b>0.11</b>	<b>23.19</b>	<b>22.41</b>	<b>3.40</b>	<b>0.89</b>	<b>0.11</b>	<b>54.43</b>

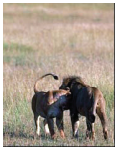
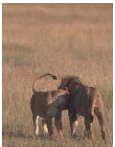
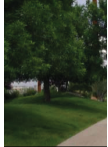




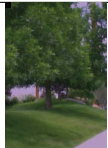
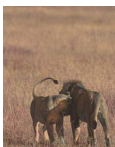
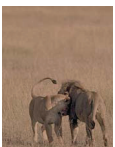




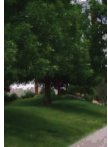
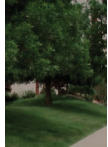


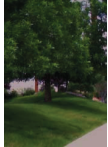
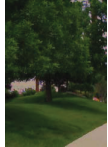


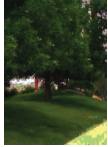
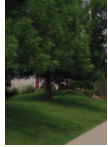
the missing algorithm [7], it was not possible to find a public implementation to guarantee a fair comparison. However, the algorithm presented in [7] did not reach the best performance in none of the tests presented in [12].

The evaluation parameters, i.e., *color similarity* (CS) and *structural similarity* (SS) were taken from [12]. For a better comparison of the tested methodologies, the average processing time taken to correct one image is also presented. Although results of both CS, SS and time are presented, the CS score is the most important parameter, since it evaluates how well a color correction algorithm is able to balance the colors in the target image so that they match the ones in the source image (see details in [12]).

Table 1 shows the average CS and SS scores of the eight methods used for comparison, as well as of the approach proposed in the current paper. Analyzing Table 1, two different classes of methods may be identified: fast algorithms #1, #2, #3, #4, #5 and #6, which have processing times under one second but have limited CS scores; and highly effective algorithms #7 #8 #9 and #10 (the proposed approach), which require more time to get the highest CS scores. Note that this CS score corresponds to a logarithmic scale (see details in [12]). Results show that the proposed approach has the highest average CS scores for both the synthetic and real data sets. Furthermore, the proposed approach presents some of the lowest values of standard deviation of CS, which accounts for a smaller variation of CS scores throughout the images in the data sets. This is also a very important remark since it accounts for the reliability and robustness of our algorithm. The proposed approach is also much faster than two of the highest scoring methods (#7 and #8).

The results presented in Table 1 are different in value from the ones presented in [12] because there is a different registration. Nonetheless, the results presented

**Table 2.** The output of the comparative methods and the proposed approach (alg. #10) for two images in the data set. The image pairs are shown on the top of the table. Below each image the CS and SS scores are displayed. For image *Synthetic #34*, algorithm #9 achieves the highest CS score. In the case of *Real #6*, the proposed approach outperforms all other methods.

Synthetic #34		Real #6	
			
Source	Target	Source	Target
Alg.; CS; SS	Alg.; CS; SS	Alg.; CS; SS	Alg.; CS; SS
			
#1 ; 17.3 ; 1.00	#2 ; 19.8 ; .98	#1 ; 12.2 ; 1.0	#2 ; 18.3 ; .88
			
#3 ; 16.9 ; 0.93	#4 ; 16.2 ; 0.94	#3 ; 13.1 ; 0.40	#4 ; 12.9 ; .38
			
#5 ; 32.8 ; 0.84	#6 ; 33.0 ; 0.86	#5 ; 21.9 ; 0.58	#6 ; 21.9 ; .63
			
#7 ; 35.4 ; 0.83	#8 ; 35.2 ; 0.83	#7 ; 22.2 ; 0.65	#8 ; 22.2 ; 0.59
			
#9 ; <b>36.9</b> ; 0.83	#10 ; 36.1 ; 0.82	#9 ; 20.5 ; 0.57	#10 ; <b>22.7</b> ; 0.58



in the current paper are consistent with those in [12], where the best average CS scores were also from algorithms #7 #8 and #9.

Table 2 gives some qualitative results. Here it is also possible to verify that the proposed approach shows the greatest similarity with the reference source image when compared to the other eight algorithms.

## 4 Conclusions

This paper proposes to use a single step multi-dimensional probabilistic segmentation of the three color channels of an image in order to perform color correction. The color distribution of the images is modelled as a 3D mixture of Gaussian components. The proposed approach is compared with several state of the art algorithms used from color correction. In addition, a large set of images, previously used in [12], are employed to assess the effectiveness of the color correction algorithms. Furthermore, the evaluation metric is taken from a recent performance evaluation in color correction. The joint segmentation of the three channel color reduces processing time from similar single channel methods and avoids cross channel artifacts that may appear due to an independent color correction of each channel separately. The proposed approach obtained the highest average CS scores and is amongst the lowest in CS standard deviation, which definitely makes it a technique to take into account for devising color correction algorithms. Results show that 3DGMM may be successfully applied to color correction with effectiveness that overcomes the current state of the art.

**Acknowledgments** The authors would like to thank the authors of [12], in particular Dr. Wei Xu, for granting access to the data-sets and implementations of other color correction algorithms. This work was supported by the Portuguese Foundation for Science and Technology under grant SFRH/43203/2008 and the Spanish Government under project TIN2011-25606 and research programme Consolider Ingenio 2010: MIPRCV (CSD2007-00018).

## References

1. Brown, M., Lowe, D.G.: Automatic panoramic image stitching using invariant features. *International Journal of Computer Vision* 74, 59–73 (August 2007), <http://portal.acm.org/citation.cfm?id=1265138.1265141>
2. Fecker, U., Barkowsky, M., Kaup, A.: Histogram-based prefiltering for luminance and chrominance compensation of multiview video. *IEEE Transactions on Circuits and Systems for Video Technology* 18(9), 1258–1267 (September 2008)
3. Jia, J., Tang, C.K.: Image registration with global and local luminance alignment. In: *Proceedings of the Ninth IEEE International Conference on Computer Vision - Volume 1*. pp. 156–163. Washington, DC, USA (October 2003)
4. Jia, J., Tang, C.K.: Tensor voting for image correction by global and local intensity alignment. *IEEE Transactions on Pattern Analysis and Machine Intelligence* 27(1), 36–50 (January 2005)

5. Kim, S.J., Pollefeys, M.: Robust radiometric calibration and vignetting correction. *IEEE Transactions on Pattern Analysis and Machine Intelligence* 30(4), 562–576 (April 2008)
6. Litvinov, A., Schechner, Y.Y.: Radiometric framework for image mosaicking. *Journal of the Optical Society of America* 22(5), 839–848 (May 2005), <http://josaa.osa.org/abstract.cfm?URI=josaa-22-5-839>
7. Pitie, F., Kokaram, A.C., Dahyot, R.: N-dimensional probability density function transfer and its application to colour transfer. *Proceedings of the Eleventh IEEE International Conference on Computer Vision* 2, 1434–1439 (October 2005)
8. Reinhard, E., Ashikhmin, M., Gooch, B., Shirley, P.: Color transfer between images. *IEEE Computer Graphics and Applications* 21, 34–41 (October 2001)
9. Tai, Y.W., Jia, J., Tang, C.K.: Local color transfer via probabilistic segmentation by expectation-maximization. In: *Proceedings of the IEEE Conference on Computer Vision and Pattern Recognition*. pp. 747–754 (June 2005)
10. Tsin, Y., Ramesh, V., Kanade, T.: Statistical calibration of ccd imaging process. In: *Proceedings of the Eighth IEEE International Conference on Computer Vision*. vol. 1, pp. 480–487 vol.1 (2001)
11. Xiao, X., Ma, L.: Color transfer in correlated color space. In: *Proceedings of the ACM International Conference on Virtual Reality Continuum and its Applications*. pp. 305–309 (June 2006), <http://doi.acm.org/10.1145/1128923.1128974>
12. Xu, W., Mulligan, J.: Performance evaluation of color correction approaches for automatic multi-view image and video stitching. In: *Proceedings of the IEEE Conference on Computer Vision and Pattern Recognition*. pp. 263–270 (June 2010)
13. Zhang, M., Georganas, N.D.: Fast color correction using principal regions mapping in different color spaces. *Real-Time Imaging* 10(1), 23–30 (February 2004), <http://www.sciencedirect.com/science/article/B6WPR-4BBMT85-1/2/95db47c705c7790b98db4e9692bf930c>
14. Zheng, Y., Yu, J., Kang, S.B., Lin, S., Kambhamettu, C.: Single-image vignetting correction using radial gradient symmetry. In: *Proceedings of the IEEE Conference on Computer Vision and Pattern Recognition*. pp. 1–8 (June 2008)